Biophysical Chemistry, 47 (1993) 123–138
Elsevier Science Publishers B.V., Amsterdam

BIOCHE 01759

A molecular mechanism of conformational gating of electron transfer in photosynthetic reaction centra

Bo Cartling

Department of Theoretical Physics, The Royal Institute of Technology, S-100 44 Stockholm (Sweden)

(Received 7 October 1992; accepted 12 February 1993)

Abstract

A mechanism based on conformational control of electron transfer provides a reinterpretation of the observed temperature dependence of electron transfer from cytochrome c to the special pair of bacteriochlorophylls in the reaction center of several photosynthetic bacteria. More generally, it constitutes an alternative contribution to the temperature dependence of electron transfer reactions in biological systems compared to the vibronic coupling and parallel path mechanisms. Starting from the crystallographic structure of the reaction center of *Rhodopseudomonas viridis*, a detailed molecular mechanism of conformational gating of electron transfer is derived by studies of conformational states and electronic structure. The low temperature, unactivated, electron transfer is assigned to a direct, superexchange, mechanism involving intermediate orbitals on a bridging tyrosine. In the high temperature, activated, region, hydrogen bond formation and proton transfer between the bridging tyrosine and an asparagine residue, in a high energy conformational state of the reaction center, makes sequential electron transfer dominate the rate. This mechanism predicts the formation of a neutral tyrosine radical during electron transfer, which should be possible to detect by timeresolved spectroscopy. The mechanism also is of interest with respect to coupling of electron and proton transfer, gating of electron transfer in biological energy transduction, the role of bridging aromatic amino acids in long-range electron transfer, and molecular electronic devices.

Keywords: Conformational gating of electron transfer; Coupled electron and proton transfer; Bridged electron transfer; Electron transfer temperature dependence; Photosynthetic reaction centra; *Rhodopseudomonas viridis*

1. Introduction

Electron transfer processes are vital to living organisms, one of the most important contexts in which they occur being biological energy transduction [1]. In photosynthesis, as well as in respiration, a sequence of electron transfer steps is primary in the reactions by which energy from an external source is transformed for storage and utilization. The elucidation of the mechanisms of electron transfer in biological systems therefore has been the objective of extensive investigations over several decades, see Refs. [2–8] for reviews and current status. The interest in biological energy conversion systems also is stimulated by the quest of achieving their efficiency in artificial systems. More recently, great interest in electron transfer processes also has arisen for the design of molecular electronic devices.

Particularly valuable insight into the mechanisms of electron transfer reactions is provided by the temperature dependence of their reaction

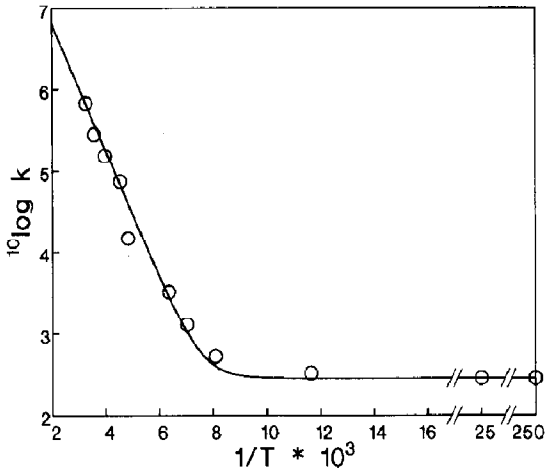

Fig. 1. The rate constant $k(s^{-1})$ of electron transfer from cytochrome c to the photoionized special pair of bacteriochlorophylls in the reaction center of *C. vinosum* vs. absolute temperature T(K). Circles represent experimental values (2), and the curve is obtained by the model described in the text.

rates. A striking temperature dependence of the electron transfer from cytochrome c to the photoionized special pair of bacteriochlorophylls in the reaction center of the photosynthetic bacterium *Chromatium vinosum* was observed by Chance and DeVault [9]. The electron transfer is nearly temperature independent below 120 K and thermally activated above, see Fig. 1. Similar types of temperature dependence have then been observed for this reaction in other photosynthetic bacteria, such as *Rhodobacter sphaeroides* [10] and *Rhodopseudomonas viridis* ([11–13]; G. Neshich, D. DeVault and C.A. Wraight, personal communication). This particular behaviour has had a large impact on the development of electron transfer theory.

The principal interpretations have been based on the vibronic coupling mechanism, i.e. vibrationally assisted electron tunneling [14–16], see Ref. [2] for a review of the early formulations. Certain nuclear degrees of freedom are assumed to be coupled to the electronic transition. A separation of the nuclear and electronic degrees of freedom by the Born–Oppenheimer approximation results in a factorization of the reaction rate into nuclear and electronic parts. The nuclear factor derives from the thermally averaged Franck–Condon factors, i.e. overlaps of nuclear wavefunctions. The electronic factor is determined by the interaction matrix element between initial and final electronic states. The temperature dependence of the reaction rate is ascribed to the nuclear factor. At high temperatures an activated rate expression results from both quantum and classical treatments of the nuclear motion. At temperatures below that corresponding to the lowest frequency of coupled nuclear modes, the reaction proceeds by temperature independent nuclear tunneling. The vibronic coupling model has subsequently undergone developments, e.g. with respect to the inclusion of the coupling between the reaction coordinates and the bath of other nuclear modes, producing friction for motion in the reaction coordinates [17–19]. The applicability of classical vs. quantum descriptions of the nuclear dynamics has been investigated [20].

More recently, it has been realized that certain parameters which result from a vibronic coupling analysis of the experimental data on *C. vinosum*, in particular the nuclear reorganization energy and the electronic interaction matrix element, assume unrealistic values [21,22]. An alternative interpretation has then been forwarded based on parallel electron transfers from two distinct hemes of the cytochrome c [21–23]. The high temperature region is proposed to be dominated by thermally activated electron transfer from a high potential heme and the low temperature region by nearly activationless electron transfer from a low potential heme. It was shown in Ref. [24] that the parallel path model cannot account for all experimental observations. Whereas the cytochrome c subunit of both *C. vinosum* and *Rps. viridis* contains four hemes, it only has a single heme in *Rb. sphaeroides* and yet the cytochrome c oxidation in this bacterial reaction center shows the same type of temperature dependence as in the others [10]. Recently, the electron transfer from a high potential heme in the cytochrome c to the special pair of bacteriochlorophylls in *Rps. viridis* has been resolved and again shows a similar type of temperature dependence ([11–13]; G. Neshich, D. DeVault and C.A. Wraight, personal communication).

The present paper is based on an extension of the electronic–vibrational coupling model by electronic-conformational coupling [25]. In Ref. [24] it was shown that a mechanism based on conformational control of electron transfer can account for the observed temperature dependence of the cytochrome c oxidation in bacterial photosynthetic reaction centra. A specific molecular mechanism of such conformational control in *Rps. viridis* has been preliminarily reported [26]. The present paper describes the detailed molecular mechanism of conformational gating of electron transfer, and accounts for the underlying calculations of conformational states as well as of electronic interaction matrix elements, in *Rps. viridis*. The principles of conformational gating of electron transfer are briefly outlined in Section 2. The calculations of conformational states and electronic structure are described in Sections 3 and 4, respectively. The resulting molecular mechanism and its implications are discussed in Section 5. Suggestions for further experimental and theoretical investigations are included in Section 6.

2. Conformational gating of electron transfer

The electronic–vibrational coupling model of electron transfer [2,14–16] was extended by electronic–conformational coupling by means of a decomposition of the nuclear degrees of freedom into vibrational and conformational types for the purpose of formulating a model of biological energy transduction [25]. A mechanism of conformational gating of electron transfer was introduced to account for the low dissipation in energy transducing processes [25]. The influence of conformational transitions on electron transfer kinetics was studied by a stochastic model of protein dynamics [25]. Conformational control of electron transfer is not restricted to such conformational degreees of freedom that are directly coupled to electronic transitions, i.e. shift equilibrium between electronic states. As discussed in Ref. [24], the state of the intervening medium between the electron donor and acceptor can affect the electron transfer rate. Conformational influence on electron transfer can occur via the nuclear factor of the reaction rate, e.g. via the activation and reorganization energy parameters of the vibronic coupling theory, but also via the electronic factor of the reaction rate, i.e. the electronic interaction matrix element between initial and final states. The internal dynamics of proteins can be decomposed into transitions between and fluctuations within conformational states. The existence of a manifold of conformational states of proteins is well established both experimentally [27–29] and theoretically [30]. A particular type of conformational transition is that primarily characterized by an altered location and orientation of a bridging group between the electron donor and acceptor.

A bridging group can assist long range electron transfer by two different mechanisms, direct and sequential. In the direct mechanism, the electronic coupling between the initial and final states is enhanced by superexchange via electronic states of the bridge. The resulting interaction matrix element is given by perturbation theory as

$$V_{da} = \sum_i \frac{V_{di} V_{ia}}{\Delta E_i}, \qquad (1)$$

where i denotes a bridge orbital, V_{di} and V_{da} interaction matrix elements between the states indicated by subindices, and ΔE_i the difference in energy of the tunneling electron and bridge orbital i. The sum over intermediate states runs over occupied and unoccupied bridge orbitals, corresponding to hole and electron conduction, respectively. The electronic coupling between donor and acceptor increases with decreasing ΔE_i. In the limit where one $\Delta E_i \to 0$, the sequential type of electron transfer is approached, in which the electron or hole actually resides on the bridge. One situation where the discrimination between these two mechanisms has been extensively investigated is the primary charge separation between the special pair of bacteriochlorophylls and one of the bacteriopheophytins in bacterial photosynthetic reaction centra, where an accessory bacteriochlorophyll is a potential bridge [31,32]. The observation of an anion radical of this accessory bacteriochlorophyll has recently been reported in *Rb. sphaeroides* [33,34]. Conse-

quences on the overall electron transfer kinetics in sequential transfer due to vibrational relaxation of the intermediate state have recently been addressed [35,36].

Conformational control of electron transfer reactions can impose a temperature dependence of the rate constant in two different ways depending on the relative rates of the conformational and electronic transitions. If the electron transfer intrinsically is fast in one conformational state, e.g. if it is nearly adiabatic, so that the equilibrium distribution between conformational states among systems in the initial electronic state is disturbed, the resulting electron transfer rate is limited by conformational transitions to this state. The thermal activation of such transitions is then underlying the temperature dependence of the apparent electron transfer rate. In the alternative situation, the conformational transitions are sufficiently rapid to maintain a thermal equilibrium distribution between conformational states among systems in the initial electronic state. The resulting electron transfer rate then is given by

$$k(t) = \sum_{i=1}^{N} p_i(T) k_i(T), \qquad (2)$$

where $p_i(T)$ is the probability of state i, $k_i(T)$ the electron transfer rate in state i and N the total number of states. In a canonical ensemble the equilibrium $p_i(T)$ are given by the Boltzmann distribution

$$p_i(T) = \frac{1}{Z(T)} \exp(-E_i/k_B T), \quad i = 1, \ldots, N \qquad (3)$$

where $Z(T)$ is the partition function and E_i the free energy of state i. The $k_i(T)$ can in principle be obtained by vibronic coupling theory and may be less temperature dependent than the $p_i(T)$. In a system with two conformational states, for which the intrinsic electron transfer rate constants are temperature independent, and with an energy difference larger than $k_B T$ the resulting rate is approximately given by

$$k(T) = k_1 + k_2 \exp[-(E_2 - E_1)/k_B T]. \qquad (4)$$

Conformational gating of electron transfer results when the electron transfer rate in one state exceeds that in other states. We will now proceed to investigate a photosynthetic reaction center with respect to possible conformational control of electron transfer underlying its observed temperature dependence.

3. Conformational states

Detailed studies of protein states and dynamics in photosynthetic reaction centra are made possible by the X-ray crystallographic structure determinations, first accomplished on the reaction center of the photosynthetic bacterium *Rhodopseudomonas viridis* [37,38]. The electron donor and acceptor groups of the presently studied electron transfer step are the cytochrome c and the special pair of bacteriochlorophylls. The cytochrome c subunit contains four hemes and is hydrophobically linked to the L and M subunits embedding the special pair. The heme proximal to the special pair has a high redox potential and the other ones low, high and low potentials in order from the special pair [39]. An aromatic amino acid, a tyrosine at the end of an α-helical section of the connection between membrane penetrating α-helices of the L subunit, is located halfway between the centra of the proximal heme of the cytochrome c and the special pair of bacteriochlorophylls. This residue, tyrosine L-162, therefore is interesting to investigate with respect to a possible role in bridging the electron transfer between these centra, which are 20 Å apart. An X-ray crystallographic structure determination is also available for the reaction center of the photosynthetic bacterium *Rhodobacter sphaeroides* [40,41]. In this species, the cytochrome c is a single heme subunit and it does not form such a strong complex with the L and M subunits as is the case in *Rps. viridis*. The binding sites of the subunits are, however, known and a docking structure has been determined [41]. Also in *Rb. sphaeroides* there is a tyrosine L-162 located midway between the heme of the cytochrome c subunit and the special pair of bacteriochlorophylls. In the photosynthetic bacterium *C. vinosum* the cytochrome c subunit contains four hemes as in *Rps. viridis*, but the structure of the reaction

center has not been determined. As mentioned in Section 1, all these three species show a similar type of temperature dependence of the cytochrome c oxidation by the photoionized special pair of bacteriochlorophylls. In *Rps. viridis* the kinetics of the electron transfer from the proximal high potential heme to the special pair is resolved under conditions maintaining the low potential hemes oxidized ([11–13]; G. Neshich, D. DeVault and C.A. Wraight, personal communication). The measured reaction rate in *C. vinosum* refers to the oxidation of a low potential heme, but the electron transfer between the proximal high potential heme and the special pair is rate limiting due to rapid interheme electron transfer [42].

A gating mechanism is based on transitions between conformational states with different electron transfer rates. The position and orientation of the aromatic ring of the bridging tyrosine, which may affect its electron transfer capability, are largely determined by the dihedral angles χ_1 and χ_2, describing rotation around the $C_\alpha - C_\beta$ and $C_\beta - C_\gamma$ bonds, respectively. An energy surface in the conformational space spanned by χ_1 and χ_2 of the tyrosine L-162 in *Rps. viridis* is determined by energy minimizations with respect to all other degrees of freedom at constrained values of χ_1 and χ_2. Steepest descent energy minimizations are performed by means of the GROMOS87 program system [43], which also defines the interaction function parameters. The system treated includes all atoms within a sphere of radius 16 Å and centered at the crystal position of the tyrosine C_γ atom. Aliphatic CH, CH_2, and CH_3 groups, as well as aromatic CH groups, are treated as extended carbon atoms, which makes the total number of atoms equal to 1078. Neither bond lengths nor bond or dihedral angles are constrained. Non-bonded interactions, i.e. Coulomb and van der Waals interactions, are completely included for interatomic distances below a cutoff at 10 Å, and the list of non-bonded interactions is updated every 20 steps of the energy minimization process. In addition, Coulomb interactions are included for atoms further apart than this cutoff but closer than 20 Å and at positions updated at the same time as the list of non-bonded interactions is. The parameters of the non-bonded interactions are determined as to include the effects of hydrogen bonding implicitly. The molecular topology of the bacteriochlorophyll group, defining its intramolecular interactions, is not included in the GROMOS87 system and has been added, with the phytyl chain substituted by a methyl group. The topology of the heme group has been extended to account for the two covalent thioether linkages between the vinyl side chains and cysteine sulfurs of the cytochrome c subunit and also for the axial ligation of a methionine and a histidine residue. In the crystal structure, which is obtained with the membraneous environment substituted by detergent molecules, some water molecules have been identified. It is not clear to what extent they represent the *in vivo* situation, in particular for the hydrophobic region studied here, where the cytochrome c forms a complex with the subunits L and M embedded in a membrane. During an energy minimization the crystal water molecules do not retain their localizations. For these two reasons water molecules are not included. The vacuum environment implies that charges have to be compensated locally, i.e. by charges on nearby atoms, to simulate their screening. As a boundary condition, atoms within a 2 Å thick shell inside the outer spherical boundary are restrained to their crystal positions by harmonic forces. In addition, the acetyl groups of the bacteriochlorophylls are similarly restrained for a more realistic distribution of electron density between the two bacteriochlorophylls of the special pair in their highest occupied molecular orbitals, as determined by the quantum chemical method described in Section 4.

The nearest neighbour interactions make an energy surface of a tyrosine residue typically have three minima with respect to χ_1, spaced by approximately 120° and near doubly degenerate due to the approximate symmetry with respect to χ_2-rotations of 180°. In the reaction center of *Rps. viridis* one of the three minima is not present because the non-bonded interactions between the tyrosine and the edge of the proximal heme of the cytochrome c dominate over those local interactions that would define this minimum. In Ref.

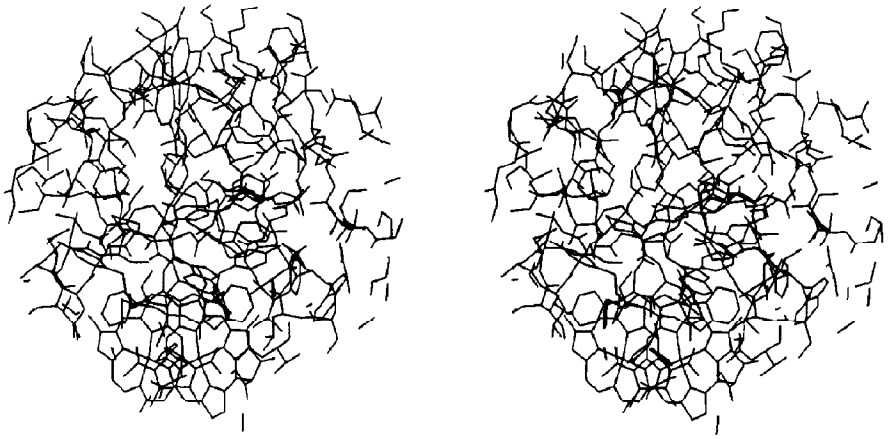

Fig. 2. Stereoscopic view of the conformational state 1. The part of the reaction center of *Rps. viridis* included in the structural calculations is shown. The proximal heme of the cytochrome c is located at the top, and the special pair of bacteriochlorophylls at the bottom. The tyrosine L-162 residue of the L subunit is at the center.

[24] the presence of a second conformational state was reported based on analogous calculations on a smaller system than the presently studied. Starting from the coordinates of this state and allowing complete relaxation in the present system results in a conformational state which we will refer to as state 2. By performing energy minimizations at successive χ_1-values and constant χ_2 towards the principal minimum, followed by complete relaxation of all degrees of freedom at this minimum, the ground state, state 1, is reached. Stereoscopic projections of the specified part of the reaction center in the two conformational states are shown in Figs. 2 and 3. The energy difference between state 2 and 1 is 0.58 eV, χ_1 shifts from $-73°$ in state 1 to 42° in state 2, i.e. by 115°, and χ_2 from $-57°$ to $-79°$. The completely relaxed state 1 can be compared to the unrelaxed crystal structure, in which χ_1 and χ_2 are $-82°$ and $-54°$, respectively, and the position of a phenylalanine C-253 of the cytochrome c subunit is shifted with respect to its χ_1. The small differences to values reported in Ref. [24] are due to the larger size of the system treated in the present study.

The orientation of the aromatic ring of the tyrosine, relative to the proximal heme of cytochrome c and the special pair of bacterio-

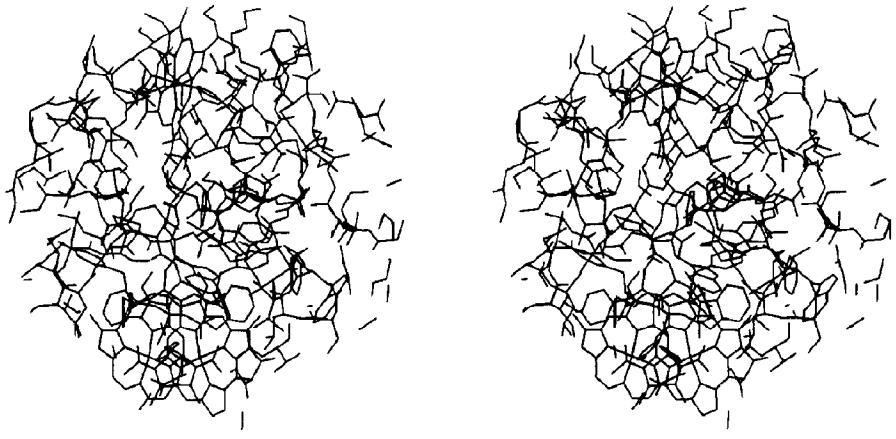

Fig. 3. As Fig. 2, but for the conformational state 2. Note the different orientation of the aromatic ring of the tyrosine L-162 residue at the center, as compared to that in state 1.

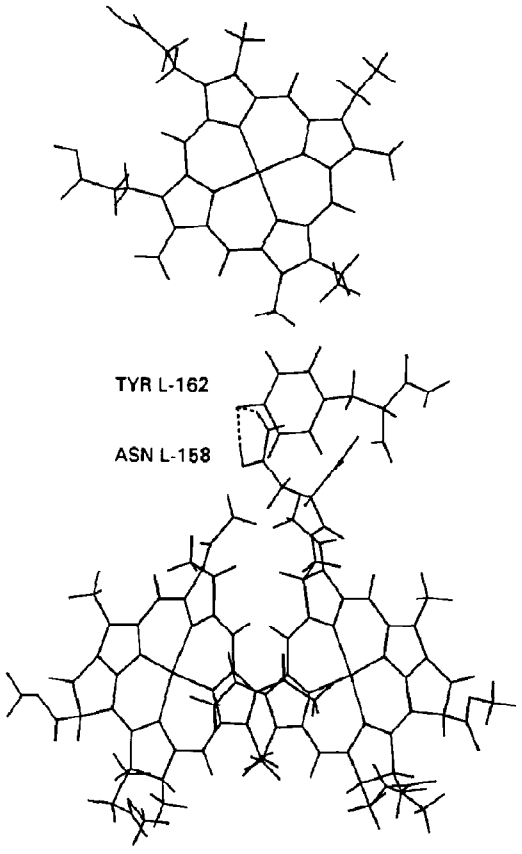

Fig. 4. Part of the reaction center of *Rps. viridis* in conformational state 2, including the proximal heme of cytochrome c (top), the special pair of bacteriochlorophylls (bottom), and the tyrosine L-162 and asparagine L-158 residues (labelled at the center). The hydrogen bonds discussed in the text are indicated by dashed lines.

chlorophylls, differs between the two conformational states, cf. Figs. 2 and 3, in a way as to increase the overlap in state 2 of the molecular π-orbitals involved in the electron transfer. In particular, the overlap between the tyrosine highest occupied π-orbital and the corresponding of the special pair improves via the C_{3C}–C_{AC}–C_{BC} sidechains of the bacteriochlorophylls stretching like arms towards the tyrosine ring. Of more importance, however, is the influence on the orbital energies of the tyrosine by the following circumstances. In state 2, hydrogen bond formation between the tyrosine and an asparagine residue in the L subunit, L-158, see Fig. 4, is enabled, whereas in state 1 there is no hydrogen bond partner for the tyrosine in the protein. The oxygen atoms of the tyrosine hydroxyl and the asparagine amide are 2.75 Å apart in state 2, which is optimal for a hydrogen bond [44]. A transfer of the proton in this hydrogen bond to the hydrogen acceptor, the oxygen of the asparagine amide, stabilizes a second hydrogen bond. The latter is between the nitrogen of the asparagine amide, serving as a hydrogen donor, and the oxygen of the tyrosine hydroxyl. The distance between these atoms is 3.09 Å, optimal for this type of hydrogen bond [44]. The stabilization of the second hydrogen bond provides driving force for the proton transfer. The occurrence of hydrogen bond formation and proton transfer is supported by observations on the plant photosystem II reaction center to be discussed in Section 5. The hydrogen bonds and, more importantly, the proton transfer in state 2 have a considerable influence on the electronic structure of the tyrosine residue, and thus on its bridging properties for electron transfer, and this is the subject of the next section.

4. Electronic structure

We are interested in determining the electronic interaction matrix element of the electron transfer steps involved in the different possible mechanisms. In the direct, superexchange, mechanism, the donor and acceptor states are localized to the cytochrome c proximal heme and special pair of bacteriochlorophylls, respectively. In a sequential mechanism the donor and acceptor are the tyrosine and special pair, respectively, for the first electron transfer step, and the cytochrome c proximal heme and tyrosine, respectively, for the second step. The objective is to compare the interaction matrix elements determining the electron transfer rates of the various steps for the two different conformational states, states 1 and 2.

For the calculation of electronic matrix elements of long-range electron transfer reactions, semi-empirical quantum chemical methods have proven useful [45–48]. The basic approach used

here is to determine an interaction matrix element V_{da} from the energy splitting Δ at an avoided crossing of the energy surfaces of the electronic states involved, where $\Delta = 2V_{da}$. The initial photoionization of the special pair of bacteriochlorophylls implies that the electronic states of interest are excited charge transfer states. We denote the proximal heme of cytochrome c by C, the special pair by P, the tyrosine by T and the acceptor of the initially photoexcited electron from the special pair by A. The direct superexchange electron transfer from C to P^+ then occurs at the avoided crossing of the energy surfaces of the CTP^+A^- and C^+TPA^- states. The first step of the sequential mechanism involves the CTP^+A^- and CT^+PA^- states, and the second step the CT^+PA^- and C^+TPA^- states. The initially excited state of the special pair has a lifetime of about 3 ps in *Rps. viridis* [49], whereafter the excited electron is transferred to, consecutively, one of the bacteriopheophytins, a menaquinone, and, finally, a ubiquinone. The lifetime of the excited state of charge separation between the special pair and a bacteriopheophytin in *Rps. viridis* is about 170 ps and not temperature dependent [50]. This is much shorter than the time constants of the cytochrome c oxidation by the special pair, and we therefore select one of the quinones, the menaquinone, as the acceptor A. The choice of A is not critical because the interaction matrix elements of interest here involve states localized on C, T or P.

The quantum chemical calculations are performed with the CNDO method [51–53] with parameters obtained as described in Ref. [47]. The one-center electron repulsion integrals are determined non-empirically from atomic Hartree–Fock–Slater calculations based on a local density energy functional. This procedure generates parameters which are similar to those of the spectroscopic CNDO version, CNDO/S [52], for H, C, N and O atoms, but it allows the inclusion of all types of atoms. The two-center electron repulsion integrals are obtained by the Mataga–Nishimoto approximation [54,55]. The one-electron Coulomb integrals are obtained empirically from averages of ionization energy and affinity, and the resonance integrals, finally, by the Wolfsberg–Helmholtz approximation [56]. This method has been applied to the primary charge separation between the special pair of bacteriochlorophylls and a bacteriopheophytin in the reaction center of *Rps. viridis* [47].

The size of the system for the quantum chemical calculations has to be reduced from that of the conformational studies. The proximal heme of the cytochrome c, the special pair of bacteriochlorophylls and three intervening amino acids as well as the acceptor, menaquinone, are included. The amino acids are tyrosine L-162 and asparagine L-158 of the L subunit and phenylalanine C-253 of the cytochrome c subunit. Peripheral atoms of the heme and the special pair outside the spherical boundary of the conformational studies are included at their crystal positions. The crystal coordinates are also used for the menaquinone. Those hydrogens that were included in extended atoms in the conformational studies have to be added separately, which results in the total number of atoms of 330. The total number of electrons and orbitals are 944 and 894, respectively. The convergence criterion of the self-consistent field iterations is a relative change of the total electronic energy less than 5×10^{-12}. The excited charge transfer states involved in the different electron transfer steps, as discussed above, are obtained by means of the configuration interaction technique. The number of lowest energy singly excited configurations included is 100 and has been checked to provide convergence by calculations with 200 configurations for both direct and sequential matrix elements.

The reaction field from the surroundings of any center induced by changes of the charge state is simulated by the introduction of charged Born spheres [57]. The reaction field energy is approximately given by the expression

$$E = \frac{1}{2}\left(1 - \frac{1}{\varepsilon}\right)\frac{Q}{r} \qquad r > a, \tag{5}$$

$$E = \frac{1}{2}\left(1 - \frac{1}{\varepsilon}\right)\frac{Q}{a} \qquad r \leq a, \tag{6}$$

where ϵ is the dielectric constant of the protein medium, a is the radius of the Born sphere and

Q its charge. The radius is chosen to be 5, 4, 8 and 4 Å for the C, T, P and A groups, respectively. The reaction field charge of the ionized menaquinone, A^-, is put equal to $+1$. The initial excited state, of any of the electron transfer steps we are interested in, has a positively charged acceptor, which should have a reaction field charge of -1. Analogously, the final excited state of an electron transfer step should have a reaction field charge of -1 at the donor due to its positive charge. The avoided crossing of these two excited states is obtained by varying the donor and acceptor Born charges maintaining their sum equal to -1. This procedure implies that the effect of any other reaction coordinate than the polarization of the surrounding medium is substituted by the effect of the latter. It has been shown that electronic matrix elements are not sensitive to the precise way in which an avoided crossing of states is obtained, and that the approximation of reaction fields by charged Born spheres provides matrix elements in good agreement with experimental observations, for long-range electron transfer in biological systems [47,48]. The choice of dielectric constant ε is not critical, since a change can be compensated by an altered charge Q. That this holds true even with the constrained total charge has been verified by calculations with $\varepsilon = 6$ and $\varepsilon = 10$ in the present system.

In conformational state 1, the direct, superexchange, matrix element is calculated to be 2.9×10^{-6} eV. The sequential mechanism cannot be operative because the highest occupied π-orbital of the tyrosine is located about 2.4 eV below the average of the energies of the highest occupied orbitals of the cytochrome c proximal heme and the special pair of bacteriochlorophylls. This implies that the energy of the CT^+PA^- state is too high relative to those of the CTP^+A^- and C^+TPA^- states for avoided crossings involved in sequential electron transfer to be reached. In conformational state 2, the tyrosine highest occupied π-orbital is shifted in between the corresponding of the heme and the special pair, 0.2 eV of this shift being caused by the hydrogen bond formation between the tyrosine and the asparagine and the remaining, dominating, shift by the proton transfer from the tyrosine hydroxyl to the asparagine amide, as described in Section 3. This enables the sequential electron transfer mechanism, and the interaction matrix elements of the first and second electron transfer steps, from tyrosine to special pair and from heme to tyrosine, are obtained as 4.3×10^{-4} and 6.0×10^{-4} eV, respectively. The direct, superexchange, matrix element in state 2 is calculated to be 3.7×10^{-6} eV.

5. Discussion

Conformational gating of electron transfer provides a reinterpretation of the temperature dependence of the electron transfer from cytochrome c to the special pair of bacteriochlorophylls in the reaction center of several photosynthetic bacteria. More generally, it constitutes an alternative contribution to the temperature dependence of electron transfer reactions in biological systems compared to the vibronic coupling [2,14–16] and parallel path [21–23] mechanisms. In the bacterial photosynthetic reaction centra, the temperature independent branch of the electron transfer rate vs. temperature is assigned to direct electron transfer between the cytochrome c and the special pair in the conformational ground state, state 1. The bridging tyrosine group assists the electron transfer by providing intermediate orbitals in a superexchange mechanism coupling the donor and acceptor states. The temperature independent process thus can be described as electron tunneling rather than the nuclear tunneling assumed in the vibronic coupling mechanism. This is actually more in accordance with the original proposal by the investigators that first observed the remarkable temperature dependence of the cytochrome c oxidation in *C. vinosum* [9].

In the high temperature activated regime, the electron transfer proceeds by a sequential mechanism enabled in the conformational high energy state, state 2. An electron is first transferred from the tyrosine to the special pair of bacteriochloro-

phylls, and then the hole on the tyrosine is filled by an electron from cytochrome c. This does imply the formation of a tyrosine radical with a lifetime determined by the second electron transfer step. Since it is important that a proton is transferred in a hydrogen bond from the tyrosine hydroxyl to the asparagine amide, for the tyrosine highest occupied π-orbital to be suitably located for a sequential electron transfer mechanism, the tyrosine radical formed will be neutral. It should be possible to detect, and determine the lifetime of, this radical by time-resolved spectroscopy. Support for this type of mechanism is also provided by observations on the plant photosystem II reaction center. Tyrosines at sequence positions 161 and 160 of the D1 and D2 subunits, respectively, corresponding to the L and M subunits of the bacterial reaction center, serve as primary and accessory electron donors to the chlorophyll dimer. The formation of tyrosine radicals during electron transfer from the oxygen evolving complex has been detected by ESR spectroscopy [58]. By an electron spin-echo modulation study, the type of spectrum observed has been specifically assigned to a neutral tyrosine radical, in which the phenyl oxygen is hydrogen-bonded to an adjacent amino acid residue [59]. It has been proposed that the tyrosine in the D1 subunit forms a hydrogen bond to a histidine [60].

The different orientation of the tyrosine in the two conformational states is expected to influence the overlaps of the π-orbitals involved on the donor, bridge and acceptor groups and thus the magnitude of the interaction matrix elements. The overlaps are enhanced in state 2 as compared to state 1, as discussed in Section 3. A comparison of the interaction matrix elements for the direct transfer between cytochrome c and the special pair shows an increase in state 2, also due to the smaller energy difference of the transferring electron and the bridging orbitals. The difference of the rate of direct electron transfer in the two states is, however, not sufficient to account for the observed electron transfer temperature dependence by conformational control. It is for this reason that the sequential mechanism is concluded to be dominating in state 2. The intrinsic electron transfer rate in both electron transfer steps is very high, and the overall rate is limited by the conformational control of the first electron transfer step, i.e. that from the tyrosine to the special pair. The comparatively small influence of orientation on the coupling matrix elements implies that reorientation of the tyrosine around its $C_\beta - C_\gamma$ axis, as described by the dihedral angle χ_2, which may proceed without large potential barriers, does not affect the bridging capability of the tyrosine significantly.

The conformational control of electron transfer raises the question of the influence of protein dynamics. Two different situations were distinguished in Section 2 for the high temperature activated electron transfer, depending on whether the conformational equilibrium in the initial electronic state of electron transfer is maintained or disturbed by the electron transfer. The very initial electron transfer kinetics, in an experiment in which the special pair is ionized by a short laser light pulse, reflect the equilibrium distribution of conformations in accordance with eq. (4), assuming that sufficient equilibration has been allowed for in the experiment. The subsequent time course of the electron transfer reaction, however, is dependent on whether the intrinsic electron transfer rate is high enough to deplete the number of reaction centra simultaneously in the high energy conformational state and in the initial electronic state of electron transfer. The relevant rates to compare are those of the intrinsic electron transfer and of the conformational transition from the high energy state. If the former dominates, the conformational transition to reach this state will be limiting the apparent rate of electron transfer. The activation energy should then, in addition to the state energy difference, include the energy barrier of the back conformational transition, which may be low. The larger the high temperature activation energy is, the larger the intrinsic electron transfer rate in the high energy conformational state has to be for a given apparent high temperature electron transfer rate. In systems with low activation energies, such as *C. vinosum* and *Rb. sphaeroides* with observed activation energies of 0.15 and 0.1 eV [9,10], respectively, the intrinsic electron transfer rate need not be so high as to disturb the conformational equilibrium.

In *C. vinosum* the measured room temperature rate is 7.6×10^5 s^{-1} and the low temperature rate is 2.9×10^2 s^{-1} [9]. A fit of the expression in eq. (4) to the experimental data is shown in Fig. 1 and results in the values $k = 2.9 \times 10^2$ s^{-1} and $k = 2.5 \times 10^8$ s^{-1}. The observed temperature dependence indicates that there is not a large entropic contribution to the free energy difference between conformational states. In *Rps. viridis* the threshold for activated behaviour is higher, about 200 K, the activation energy is 0.43 eV, the room temperature rate 3.7×10^6 s^{-1} and the rate at 150 K 5×10^3 s^{-1} ([11–13]; G. Neshich, D. DeVault and C.A. Wraight, personal communication). Application of eq. (4) results in $k_1 = 5 \times 10^3$ s^{-1} and $k_2 = 5.6 \times 10^{13}$ s^{-1}, i.e. the intrinsic electron transfer in conformational state 2 would have to be adiabatic. From this we conclude that the apparent electron transfer rate may rather be limited by the conformational transitions to this state.

The intrinsic electron transfer rate in any given conformational state can be determined from the interaction matrix element by the vibronic coupling theory, e.g. by the Landau–Zener [61,62] expression for the non-adiabatic transition probability at an avoided crossing of energy surfaces

$$k = \frac{4\pi^2}{h} \frac{V_{da}^2}{(4\pi\lambda k_B T)^{1/2}} \exp\left(-\frac{\Delta G^\dagger}{k_B T}\right), \qquad (7)$$

where V_{da} is the electronic interaction matrix element between donor and acceptor states, λ is the nuclear reorganization energy and $\Delta G^\dagger$ the activation energy. h and k_B are the Planck and Boltzmann constants, respectively, and T the absolute temperature. In a harmonic approximation of the initial and final energy surfaces

$$\Delta G^\dagger = \frac{\lambda}{4}\left(1 - \frac{\Delta G^\circ}{\lambda}\right)^2, \qquad (8)$$

where ΔG° is the free energy difference between the initial and final states, or the driving force of the reaction. In the present system an experimental value of ΔG° is available only for the direct electron transfer between cytochrome c and the special pair, it is obtained from the difference of the redox potentials of the proximal high potential heme of the cytochrome c and the special pair as 0.15 eV [42,63]. If the intrinsic electron transfer in the different conformational states are unactivated, i.e. $\Delta G^\dagger = 0$, then $\lambda = \Delta G^\circ$ according to eq. (8). With this assumption, the experimental value of the rate in *Rps. viridis* at 150 K, 5×10^3 s^{-1}, corresponds to a coupling matrix element of 2.9×10^{-7} eV to be compared to the superexchange matrix element obtained above for conformational state 1, 2.9×10^{-6} eV. As discussed above, in the activated region the observed rate may reflect conformational transitions to the conformational state 2. The intrinsic electron transfer in this state then has to be sufficiently rapid that the conformational equilibrium in the initial electronic state of electron transfer is disturbed. The calculated interaction matrix elements of 4.3×10^{-4} and 6.0×10^{-4} eV for the tyrosine to special pair and the cytochrome c to tyrosine steps, respectively, correspond to rates 1.1×10^{10} s^{-1} and 2.2×10^{10} s^{-1} at room temperature, assuming unactivated steps and dividing the total ΔG° equally among the two steps. The large difference to the direct, superexchange, electron transfer rate at low temperatures clearly demonstrates the dramatic gating effect of the conformational transition between states 1 and 2. This conformational transition therefore functions as an electron transfer switch.

The calculated energy difference between the two conformational states, 0.58 eV, is slightly larger than the observed high temperature activation energy of electron transfer, 0.43 eV ([11–13]; G. Neshich, D. DeVault and C.A. Wraight, personal communication). The interaction function parameters used in the energy minimizations are of course of an approximate nature. In particular, the parameters of the nonbonded interactions, electrostatic and van der Waals, are determined in GROMOS87 [43] as to include the effects of hydrogen bonding only implicitly. It is therefore not possible by these means to determine the detailed energetics of the formation of the two hydrogen bonds and the proton transfer between the tyrosine and asparagine residues. The variation of the high temperature activation energy of

electron transfer between different photosynthetic bacteria may be ascribed to structural differences affecting the energy difference between the conformational states involved.

For the determination of the rates of the type of conformational transitions discussed here, a recent approach is of particular interest [64,65]. It is based on theories of stochastic processes in order to extend the time scales beyond those presently accessible by the direct molecular dynamics simulation techniques [66]. In the stochastic model, the coupling strength between a conformational reaction coordinate and the remaining degrees of freedom in the system is determined from an analysis of the short-time fluctuations. The rates of conformational transitions is determined from this coupling strength and an effective potential energy function of the reaction coordinate by means of the non-stationary solutions of the Fokker–Planck equation. The latter determines the time evolution of the probability density function in the phase space for Brownian motion. The resulting electron transfer kinetics in a system with coupled electronic and conformational transitions were investigated in Ref. [25] for different relative rates of these processes by means of coupled Smoluchowski equations.

The stochastic model of protein dynamics has been applied to conformational transitions of an aromatic amino acid in an α-helix [64,65], in particular between states primarily distinguished by different values of the dihedral angle χ_1, because of the possible significance of such conformational transitions to electron transfer. The stochastic methods make it possible to study this type of conformational transition in a realistic system such as the reaction center. The detailed analysis of *Rps. viridis* will also require more detailed experimental data on the temperature dependence of the electron transfer kinetics. An estimate of the conformational transition rate in the present system can be obtained from the curvature with respect to χ_1 of the calculated energy surface in the conformational ground state, determining the force constant, and the moment of inertia of the tyrosine around the $C_\alpha - C_\beta$ axis. This results in an estimated frequency ω of about 4×10^{12} s^{-1}. An upper limit of the transition rate can be obtained from the transition state theory as $(\omega/2\pi)\exp(-\Delta E/k_B T)$, where ΔE is the energy barrier. If ΔE is put equal to 0.43 eV, i.e. the back transition barrier is neglected, the resulting rate is 4×10^4 s^{-1} at room temperature. The reduction of the actual reaction rate compared to the transition state value is determined by the strength of coupling of the reaction coordinate to the rest of the system, or the damping constant. A method to determine the resulting rate constant, which is useful at all strengths of the damping, has been developed and applied to transitions in bistable potentials [67,68]. From a moderate reduction of the reaction rate at intermediate damping it is considerably reduced at both strong and weak damping. Whereas an intermediate damping resulted from model studies of the swinging of an aromatic amino acid in an α-helix [64,65], the estimated rate is still lower than the apparent electron transfer rate at room temperature.

The role of bridging aromatic amino acids in long-range electron transfer reactions has long been debated. A particularly large influence was detected in the cytochrome c–cytochrome c peroxidase complex, in which electron transfer is considerably faster for cytochrome c with phenylalanine or tyrosine at sequence position 82 than for the serine or glycine mutants [69]. An X-ray crystallographic structure determination of the reduced form of cytochrome c revealed conformational changes upon substitution of the native phenylalanine by serine [70]. It was then shown that it is not changes of the superexchange coupling that accounts for the different electron transfer rates, but more likely structural changes, in particular at the protein–protein interface [71]. The role of tryptophan in a superexchange mechanism of quinone reduction in photosynthetic reaction centra has been studied [72]. The formation of radicals implies a decisive influence of aromatic amino acids on electron transfer. As mentioned above, it has been observed in the plant photosystem II reaction center, but also in other systems [73]. In a recent discussion [74] it is concluded from a comparison of the redox potentials of polarizable amino acids that in particular tyrosine and tryptophan are good candidates for

ionization in both aqueous and non-polar environments.

It is interesting to contrast the present mechanism of electron gating with the conclusions of extensive investigations of other electron transfer steps in the reaction center of *Rps. viridis* by large scale molecular dynamics simulations combined with a spin–boson model of electron transfer [75–77]. There it has been concluded that the coupling between electronic and nuclear degrees of freedom is not localized to a few crucial nuclear degrees of freedom but rather is distributed over a large number. The detailed study in the present work demonstrates an occurrence of the reverse situation. Molecular dynamics simulations of the reaction center have also been combined with the dispersed polaron model of electron transfer [78–81]. Alternative roles of the bridging tyrosine, in the electron transfer step discussed in this work, have been considered. The temperature dependent amplitude of rotational fluctuations of the tyrosine was suggested to be underlying the high temperature activation via the influence on the dielectric constant of the intervening medium [82,83]. The dynamics of this tyrosine has then been studied by molecular dynamics simulations [84,85].

Conformational gating of electron transfer was introduced as a means of limiting dissipative processes in biological energy transductions [25]. Experiments on electron transfer in cytochrome oxidase have been interpreted in terms of electron gating [86]. Conformational influence on nuclear reorganization energies has been considered as an underlying mechanism [87], partly based on the argument that efficient gating via the electronic interaction matrix element would require unreasonably large changes of the distance between donor and acceptor. The conformational switch discussed in the present paper demonstrates a quite different molecular mechanism underlying electron gating, although the particular electron transfer step studied is not coupled to phosphorylation. The involvement of a proton transfer also makes the mechanism interesting with respect to coupling of electron and proton transfer, which is fundamental to biological energy transductions. The molecular mechanism of a conformational switch of electron transfer also provides guidance for the development of crucial components of molecular electronic devices.

6. Conclusions

The classical electron transfer experiment by Chance and DeVault on the temperature dependence of the cytochrome c oxidation by the photoionized special pair of bacteriochlorophylls in the reaction center of the photosynthetic bacterium *C. vinosum* [9] and analogous experiments on other bacterial reaction centra, such as *Rps. viridis* ([11–13]; G. Neshich, D. DeVault and C.A. Wraight, personal communication) and *Rb. sphaeroides* [10], are reinterpreted in terms of conformational control of electron transfer. The low temperature unactivated behaviour is ascribed to direct electron transfer between cytochrome c and the special pair, assisted by intermediate orbitals on a bridging tyrosine in a superexchange mechanism. This corresponds to electron tunneling rather than the nuclear tunneling concluded from the vibronic coupling theory. In the activated high temperature region, the rate of electron transfer by a sequential mechanism, enabled in a high energy conformational state, dominates. In *Rps. viridis*, hydrogen bond formation and proton transfer between the bridging tyrosine and an asparagine residue in the high energy conformational state shifts the highest occupied π-orbital of the tyrosine as required for the sequential electron transfer mechanism to be operative. This mechanism implies the formation of a neutral tyrosine radical, which should be possible to detect by time resolved spectroscopy, as it has been in the plant photosystem II reaction center.

Two different situations were distinguished by the relative rates of conformational and electronic transitions. The conformational equilibrium in the initial electronic state of electron transfer can be maintained or disturbed by the electron transfer. In the latter case the conformational transitions to the state with fast electron transfer are limiting the apparent electron transfer rate. A recent stochastic approach [64,65] was

concluded to be useful for the determination of the conformational transition rates, since the timescales are beyond those accessible by molecular dynamics simulations.

The existence of a conformational switch of electron transfer contrasts with the conclusion, from extensive molecular dynamics simulations combined with a spin–boson model of electron transfer on other electron transfer steps in the reaction center [75–77], that the electronic–nuclear coupling is distributed over a large number of nuclear degrees of freedom. The involvement of a proton transfer makes the mechanism of interest with respect to the coupling of electron and proton transfer, which is fundamental in bioenergetics. Conformational gating of electron transfer was introduced as a means to limit dissipative processes in biological energy transduction [25]. It is also of interest for the design of molecular electronic devices.

Further investigations of conformational control of electron transfer, both experimental and theoretical, will be important. In the bacterial reaction centra, studies by timeresolved spectroscopy to probe, and determine the lifetime of, the predicted neutral tyrosine radical during electron transfer are particularly important. It is also interesting to study the effects on electron transfer from substitution of the hydrogen-bonding tyrosine residue by a non-hydrogen-bonding residue, such as phenylalanine, by means of site-directed mutagenesis. The recently developed technique [88] of attaching redox active groups on the surface of proteins offers the possibility to select particular electron transfer pathways, so that the influence on electron transfer of particular residues and e.g. their hydrogen bonding can be studied. Theoretically, further studies of both conformational states and electronic structures, as well as studies of the protein dynamics by means of the abovementioned stochastic approach, are all important.

Acknowledgements

This work has been supported by the Swedish Natural Science Research Council. I am grateful to Sven Larsson and Anders Broo for valuable discussions and for providing a CNDO program.

References

1 W.A. Cramer and D.B. Knaff, Energy transduction in biological membranes (Springer, New York, 1990).
2 D. DeVault, Quantum-mechanical tunnelling in biological systems (Cambridge University, Cambridge, 1984).
3 R.A. Marcus and N. Sutin, Biochim. Biophys. Acta 811 (1985) 265.
4 M.K. Johnson, R.B. King, D.M. Kurtz, Jr., C. Kutal, M.L. Norton and R.A. Scott, eds., Electron transfer in biology and the solid state, Advances in Chemistry Series, vol. 226 (American Chemical Society, Washington, DC, 1990).
5 J. Jortner and B. Pullman, eds., Perspectives in photosynthesis, The Jerusalem Symposia on Quantum Chemistry and Biochemistry, vol. 22 (Kluwer, Dordrecht, 1990).
6 M.E. Michel-Beyerle, ed., Reaction centers of photosynthetic bacteria, Springer Series in Biophysics, vol. 6 (Springer, Berlin, 1990).
7 H. Sigel and A. Sigel, eds., Electron transfer reactions in metalloproteins, Metal Ions in Biological Systems, vol. 27 (Dekker, New York, 1991).
8 J.R. Bolton, N. Mataga and G. McLendon, eds., Electron transfer in inorganic, organic, and biological systems, Advances in Chemistry Series, vol. 228 (American Chemical Society, Washington, DC, 1991).
9 D. DeVault and B. Chance, Biophys. J. 6 (1966) 825.
10 T. Kihara and J.A. McCray, Biochim. Biophys. Acta 292 (1973) 297.
11 R.J. Shopes, L.M.A. Levine, D. Holten and C.A. Wraight, Photosynth. Res. 12 (1987) 165.
12 G. Neshich, D. DeVault and C.A. Wraight, Biophys. J. 55 (1989) 181a.
13 J.-L. Gao, R.J. Shopes and C.A. Wraight, Biochim. Biophys. Acta 1015 (1990) 96.
14 L.N. Grigorov and D.S. Chernavskii, Biophysics (U.S.S.R.) 17 (1972) 202.
15 J.J. Hopfield, Proc. Natl. Acad. Sci. USA 71 (1974) 3640.
16 J. Jortner, J. Chem. Phys. 64 (1976) 4860.
17 A. Garg, J.N. Onuchic and V. Ambegaokar, J. Chem. Phys. 83 (1985) 4491.
18 J.N. Onuchic, J. Chem. Phys. 86 (1987) 3925.
19 I. Rips and J. Jortner, J. Chem. Phys. 87 (1987) 2090.
20 J.N. Onuchic and P.G. Wolynes, J. Phys. Chem. 92 (1988) 6495.
21 M. Bixon and J. Jortner, J. Phys. Chem. 90 (1986) 3795.
22 M. Bixon and J. Jortner, FEBS Lett. 200 (1986) 303.
23 M. Bixon and J. Jortner, Photosynth. Res. 22 (1989) 29.
24 B. Cartling, J. Chem. Phys. 95 (1991) 317.
25 B. Cartling, J. Chem. Phys. 83 (1985) 5231.
26 B. Cartling, Chem. Phys. Lett. 196 (1992) 128.
27 R.H. Austin, K.W. Beeson, L. Eisenstein, H. Frauenfelder and I.C. Gunsalus, Biochemistry 14 (1975) 5355.
28 A. Ansari, J. Berendzen, S.F. Bowne, H. Frauenfelder,

I.E.T. Iben, T.B. Sauke, E. Shyamsunder and R.D. Young, Proc. Natl. Acad. Sci. USA 82 (1985) 5000.
29 H. Frauenfelder, F. Parak and R.D. Young, Annu. Rev. Biophys. Biophys. Chem. 17 (1988) 451.
30 R. Elber and M. Karplus, Science 235 (1987) 318.
31 R.A. Marcus, Chem. Phys. Lett. 133 (1987) 471.
32 M. Bixon, J. Jortner and M.E. Michel-Beyerle, in: Reaction centers of photosynthetic bacteria, ed. M.E. Michel-Beyerle, Springer Series in Biophysics, vol. 6 (Springer, Berlin, 1990) p. 389.
33 W. Holzapfel, U. Finkele, W. Kaiser, D. Oesterhelt, H. Scheer, H.U. Stilz and W. Zinth, Chem. Phys. Lett. 160 (1989) 1.
34 W. Holzapfel, U. Finkele, W. Kaiser, D. Oesterhelt, H. Scheer, H.U. Stilz and W. Zinth, Proc. Natl. Acad. Sci. USA 87 (1990) 5168.
35 Y.I. Kharkats and J. Ulstrup, Chem. Phys. Lett. 182 (1991) 81.
36 A.M. Kuznetsov and J. Ulstrup, Chem. Phys. 157 (1991) 25.
37 J. Deisenhofer, O. Epp, K. Miki, R. Huber and H. Michel, J. Mol. Biol. 180 (1984) 385.
38 H. Michel, O. Epp and J. Deisenhofer, EMBO J. 5 (1986) 2445.
39 G. Fritzsch, S. Buchanan and H. Michel, Biochim. Biophys. Acta 977 (1989) 157.
40 J.P. Allen, G. Feher, T.O. Yeates, H. Komiya and D.C. Rees, Proc. Natl. Acad. Sci. USA 84 (1987) 5730.
41 J.P. Allen, G. Feher, T.O. Yeates, H. Komiya and D.C. Rees, Proc. Natl. Acad. Sci. USA 84 (1987) 6162.
42 P.L. Dutton, in: Photosynthesis III, eds. A.C. Staehelin and C.J. Arntzen, Encyclopedia of Plant Physiology, vol. 19 (Springer, Berlin, 1986) p. 197.
43 W.F. van Gunsteren and H.J.C. Berendsen, GROMOS87 (Biomolecular software b.v., Groningen University, Groningen, 1987).
44 L. Stryer, Biochemistry (Freeman, San Fransisco, CA, 1981).
45 S. Larsson, J. Am. Chem. Soc. 103 (1981) 4034.
46 S. Larsson, J. Chem. Soc. Faraday Trans. II 79 (1983) 1375.
47 S. Larsson, A. Broo, B. Källebring and A. Volosov, Int. J. Quant. Chem. (Quant. Biol. Symp.) 15 (1988) 1.
48 A. Broo and S. Larsson, Int. J. Quant. Chem. (Quant. Biol. Symp.) 16 (1989) 185.
49 J. Breton, J.L. Martin, A. Migus, A. Antonetti and A. Orszag, Proc. Natl. Acad. Sci. USA 83 (1986) 5121.
50 C. Kirmaier and D. Holten, in: The photosynthetic bacterial reaction center: Structure and dynamics, eds. J. Breton and A. Verméglio, NATO ASI Series, vol. 149 (Plenum, New York, 1988) p. 219.
51 J.A. Pople, D.P. Santry and G.A. Segal, J. Chem. Phys. 43 (1965) S129.
52 J. Del Bene and H.H. Jaffé, J. Chem. Phys. 48 (1968) 1807.
53 J.N. Murrell and A.J. Harget, Semi-empirical self-consistent-field molecular-orbital theory of molecules (Wiley, London, 1972).
54 K. Nishimoto and N. Mataga, Z. Physik. Chem. 12 (1957) 335.
55 N. Mataga and K. Nishimoto, Z. Physik. Chem. 13 (1957) 140.
56 M. Wolfsberg and L. Helmholtz, J. Chem. Phys. 20 (1952) 837.
57 M. Born, Z. Physik 1 (1920) 45.
58 B.A. Barry and G.T. Babcock, Proc. Natl. Acad. Sci. USA 84 (1987) 7099.
59 R.G. Evelo, S.A. Dikanov and A.J. Hoff, Chem. Phys. Lett. 157 (1989) 25.
60 B. Svensson, I. Vass, E. Cedergren and S. Styring, EMBO J. 9 (1990) 2051.
61 L. Landau, Phys. Z. 1 (1932) 88.
62 C. Zener, Proc. R. Soc. Lond. A137 (1932) 696.
63 P.L. Dutton and R.C. Prince, in: The photosynthetic bacteria, eds. R.K. Clayton and W.R. Sistrom (Plenum, New York, 1978) p. 525.
64 B. Cartling, J. Chem. Phys. 91 (1989) 427.
65 B. Cartling, J. Chem. Phys. 94 (1991) 6203.
66 J.A. McCammon and S.C. Harvey, Dynamics of proteins and nucleic acids (Cambridge University, Cambridge, 1987).
67 B. Cartling, J. Chem. Phys. 87 (1987) 2638.
68 B. Cartling, J. Chem. Phys. 90 (1989) 1819.
69 N. Liang, G.J. Pielak, A.G. Mauk, M. Smith and B.M. Hoffman, Proc. Natl. Acad. Sci. USA 84 (1987) 1249.
70 G.V. Louie, G.J. Pielak, M. Smith and G.D. Brayer, Biochemistry 27 (1988) 7870.
71 A.M. Everest, S.A. Wallin, E.D.A. Stemp, J.M. Nocek, A.G. Mauk and B.M. Hoffman, J. Am. Chem. Soc. 113 (1991) 4337.
72 M. Plato, M.E. Michel-Beyerle, M. Bixon and J. Jortner, FEBS Lett. 249 (1989) 70.
73 G.T. Babcock, I.D. Rodriguez, C. Hoganson, P.O. Sandusky and M. El-Deeb, in: European conference on the spectroscopy of biological molecules, eds. R.E. Hester and R.B. Girling (Royal Society of Chemistry, Cambridge, 1991) p. 55.
74 S.S. Isied, in: Electron transfer reactions in metalloproteins, eds. H. Sigel and A. Sigel, Metal Ions in Biological Systems, vol. 27 (Marcel Dekker, New York, 1991) p. 1.
75 K. Schulten, H. Treutlein, A. Brünger, M. Karplus, J. Deisenhofer and H. Michel, Proc. Natl. Acad. Sci. USA 89 (1992) 75.
76 K. Schulten and M. Tesch, Chem. Phys. 158 (1991) 421.
77 D. Xu and K. Schulten, submitted.
78 A. Warshel, S. Creighton and W.W. Parson, J. Phys. Chem. 92 (1988) 2696.
79 S. Creighton, J.-K. Hwang, A. Warshel, W.W. Parson and J. Norris, Biochemistry 27 (1988) 775.
80 A. Warshel, Z.T. Chu and W.W. Parson, Science 246 (1989) 112.
81 A. Warshel and W.W. Parson, Annu. Rev. Phys. Chem. 42 (1991) 279.
82 E.W. Knapp and S.F. Fischer, J. Chem. Phys. 87 (1987) 3880.

83 S.F. Fischer and E.W. Knapp, J. Chem. Phys. 89 (1988) 3394.
84 E.W. Knapp and L. Nilsson, in: Perspectives of photosynthesis, eds. J. Jortner and B. Pullman, The Jerusalem Symposia on Quantum Chemistry and Biochemistry, vol. 22 (Kluwer, Dordrecht, 1990) p. 389.
85 E.W. Knapp and L. Nilsson, in: Reaction centers of photosynthetic bacteria, ed. M.-E. Michel-Beyerle, Springer Series in Biophysics, vol. 6 (Springer, Berlin, 1990) p. 437.
86 P. Brzezinski and B.G. Malmström, Biochim. Biophys. Acta 894 (1987) 29.
87 H.B. Gray and B.G. Malmström, Biochemistry 28 (1989) 7499.
88 B.E. Bowler, A.L. Raphael and H.B. Gray, Prog. Inorg. Chem.38 (1990) 259.